

Charts of Heat Conduction for the Stepwise Change of Surface Convection or Radiation Conditions

Yuji SANO*, Takao NISHI**, Minoru SHIBATA***
and Shinji FUJINO*.

(Received December 5, 1972)

Abstract

The temperature distribution for non-steady heat conduction in solids, where the initial temperature distribution is parabolic and the surface heat flux is controlled by fluid convection or radiation, can be expressed in the following equation, regardless of solid shapes of plates, cylinders and spheres.

$$\frac{t - t^*}{t_{0i} - t^*} = E - \frac{t_{0i} - t_{si}}{t_{0i} - t^*} E'$$

E and E' were expressed in Equations (8)~(13) for each solid shape in Table 1 and calculated by the computer for various values of parameters such as $\alpha\theta/R^2$, λ/Rh , and r/R . If the initial temperature distributions were uniform, temperature curves in solids were found to be parabolic at any time for dimensionless time $\alpha\theta/R^2 > 0.2$, regardless of solid shapes. E and E' for the center and surface of solids were shown in the charts for each solid shape. If these charts are used repeatedly with Equations (4) and (7), temperature distribution histories can be calculated easily for the case that the surface convection or radiation conditions (heat transfer coefficients and equilibrium temperatures) are changed stepwisely. Charts for E_{av} and E'_{av} , which serve to obtain the average temperatures, were also given.

For the extreme case that the heat transfer coefficient tended toward infinity and the surface temperature became closer to the equilibrium temperature, the charts for the average temperature were shown.

Introduction

Charts for calculation of temperature distribution in solids of simple shapes such as plates, cylinders, and spheres for nonsteady heat conduction, when the heat transfer of solid surface is controlled by the heat convection or radiation, were reported by many investigators such as Gurney Lurie¹⁾, Heisler,²⁾ Hottel,³⁾ etc. and quoted in various technical handbooks. But these charts are limited only to the use for the constant convection or radiation conditions and not applicable when the surface conditions are changed.

In the practical operations of heating or cooling of solids, it is occasionally

* Department of Chemical Engineering

** Sanyō Kokusaku Pulp Co. Ltd.

*** Kyōwa Hakkō Co. Ltd.

Table 1. The heat conduction equations for the condition of surface convection or radiation

Shape	Plate	Cylinder	Sphere
Heat Conduction Eq.	(1) $-\frac{\partial t}{\partial \theta} = \alpha \left(\frac{\partial^2 t}{\partial r^2} \right)$	(2) $\frac{\partial t}{\partial \theta} = \frac{\alpha}{r} \frac{\partial}{\partial r} \left(r \frac{\partial t}{\partial r} \right)$	(3) $\frac{\partial t}{\partial \theta} = \frac{\alpha}{r^2} \frac{\partial}{\partial r} \left(r^2 \frac{\partial t}{\partial r} \right)$
Initial Condition	$(t_{si} - t) / (t_{si} - t_{oi}) = \left[1 - \left(\frac{r}{R} \right)^2 \right]$	$\theta = 0$	(4) $0 \leq r \leq R$
Boundary Condition-1	$\frac{\partial t}{\partial r} = 0$	$\theta > 0$	(5) $r = 0$
Boundary Condition-2	$-\lambda \left(\frac{\partial t}{\partial r} \right) = h(t_s - t^*)$	$\theta > 0$	(6) $r = \pm R$
General Form of Solution	$\frac{t - t^*}{t_{oi} - t^*} = E - \frac{t_{oi} - t_{si}}{t_{oi} - t^*} \cdot E', \quad 0 \leq \frac{t_{oi} - t_{si}}{t_{oi} - t^*} \leq 1$		(7)
E	(8) $\sum_{k=1}^{\infty} \frac{2 \cdot \exp(-\alpha \theta u_k^2 / R^2) \cos(u_k r / R)}{m \left[\left(\frac{1}{m} \right)^2 + u_k^2 \right] \cos(u_k)}$	(10) $\sum_{k=1}^{\infty} \frac{2 \cdot \exp(-\alpha \theta u_k^2 / R^2) \cdot J_0(u_k \cdot r / R)}{m \left[\left(\frac{1}{m} \right)^2 + u_k^2 \right] \cdot J_0(u_k)}$	(12) $\sum_{k=1}^{\infty} \frac{2}{(r/R)} \cdot \frac{\exp(-\alpha \theta u_k^2 / R^2) \cdot \sin(u_k r / R)}{m \left[\left(\frac{1}{m} \right)^2 - \left(\frac{1}{m} \right) + u_k^2 \right] \sin(u_k)}$
E'	(9) $\sum_{k=1}^{\infty} \frac{2 \cdot \exp(-\alpha \theta u_k^2 / R^2) \cos(u_k r / R)}{m \left[\left(\frac{1}{m} \right)^2 + u_k^2 \right] \cos(u_k)} \times \left[1 + 2m - \left(\frac{2}{u_k^2} \right) \right]$	(11) $\sum_{k=1}^{\infty} \frac{2 \cdot \exp(-\alpha \theta u_k^2 / R^2) \cdot J_0(u_k \cdot r / R)}{m \left[\left(\frac{1}{m} \right)^2 + u_k^2 \right] \cdot J_0(u_k)} \times \left[1 + 2m - \left(\frac{4}{u_k^2} \right) \right]$	(13) $\sum_{k=1}^{\infty} \frac{2}{(r/R)} \cdot \frac{\exp(-\alpha \theta u_k^2 / R^2) \cdot \sin(u_k r / R)}{m \left[\left(\frac{1}{m} \right)^2 - \left(\frac{1}{m} \right) + u_k^2 \right] \sin(u_k)} \times \left[1 + 2m - \left(\frac{6}{u_k^2} \right) \right]$
Eq. of u_k	(14) $u_k = \cot(u_k) / m$	(15) $u_k J_1(u_k) = J_0(u_k) / m$	(16) $u_k = \left[1 - \left(\frac{1}{m} \right) \right] \cdot \tan(u_k)$
E_s	(17) $\sum_{k=1}^{\infty} \frac{2 \cdot \exp(-\alpha \theta u_k^2 / R^2)}{m \left[\left(\frac{1}{m} \right)^2 + u_k^2 \right]}$	(19) $\sum_{k=1}^{\infty} \frac{2 \cdot \exp(-\alpha \theta u_k^2 / R^2)}{m \left[\left(\frac{1}{m} \right)^2 + u_k^2 \right]}$	(21) $\sum_{k=1}^{\infty} \frac{2 \cdot \exp(-\alpha \theta u_k^2 / R^2)}{m \left[\left(\frac{1}{m} \right)^2 - \left(\frac{1}{m} \right) + u_k^2 \right]}$
E'_s	(18) $\sum_{k=1}^{\infty} \frac{2 \cdot \exp(-\alpha \theta u_k^2 / R^2)}{m \left[\left(\frac{1}{m} \right)^2 + u_k^2 \right]} \times \left[1 + 2m - \left(\frac{2}{u_k^2} \right) \right]$	(20) $\sum_{k=1}^{\infty} \frac{2 \cdot \exp(-\alpha \theta u_k^2 / R^2)}{m \left[\left(\frac{1}{m} \right)^2 + u_k^2 \right]} \times \left[1 + 2m - \left(\frac{4}{u_k^2} \right) \right]$	(22) $\sum_{k=1}^{\infty} \frac{2 \cdot \exp(-\alpha \theta u_k^2 / R^2)}{m \left[\left(\frac{1}{m} \right)^2 - \left(\frac{1}{m} \right) + u_k^2 \right]} \times \left[1 + 2m - \left(\frac{6}{u_k^2} \right) \right]$

Table 1. continued

E_0	$\sum_{k=1}^{\infty} \frac{2 \cdot \exp(-\alpha \theta u_k^2 / R^2)}{m \left[\left(\frac{1}{m} \right)^2 + \left(\frac{1}{m} \right) + u_k^2 \right] \cdot \cos(u_k)} \quad (23)$	$\sum_{k=1}^{\infty} \frac{2 \cdot \exp(-\alpha \theta u_k^2 / R^2)}{m \left[\left(\frac{1}{m} \right)^2 + u_k^2 \right] \cdot J_0(u_k)} \quad (25)$	$\sum_{k=1}^{\infty} \frac{2 \cdot u_k \exp(-\alpha \theta u_k^2 / R^2)}{m \left[\left(\frac{1}{m} \right)^2 - \left(\frac{1}{m} \right) + u_k^2 \right] \sin(u_k)} \quad (27)$
E'_0	$\sum_{k=1}^{\infty} \frac{2 \cdot \exp(-\alpha \theta u_k^2 / R^2)}{m \left[\left(\frac{1}{m} \right)^2 + \left(\frac{1}{m} \right) + u_k^2 \right] \cdot \cos(u_k)} \times \left[1 + 2m - \left(\frac{2}{u_k^2} \right) \right] \quad (24)$	$\sum_{k=1}^{\infty} \frac{2 \cdot \exp(-\alpha \theta u_k^2 / R^2)}{m \left[\left(\frac{1}{m} \right)^2 + u_k^2 \right] \cdot J_0(u_k)} \times \left[1 + 2m - \left(\frac{4}{u_k^2} \right) \right] \quad (26)$	$\sum_{k=1}^{\infty} \frac{2 \cdot u_k \exp(-\alpha \theta u_k^2 / R^2)}{m \left[\left(\frac{1}{m} \right)^2 - \left(\frac{1}{m} \right) + u_k^2 \right] \sin(u_k)} \times \left[1 + 2m - \left(\frac{6}{u_k^2} \right) \right] \quad (28)$
E_{av}	$\sum_{k=1}^{\infty} \frac{2 \cdot \exp(-\alpha \theta u_k^2 / R^2)}{m \left[\left(\frac{1}{m} \right)^2 + \left(\frac{1}{m} \right) + u_k^2 \right] \cdot \left(\frac{1}{u_k^2} \right)} \quad (29)$	$\sum_{k=1}^{\infty} \frac{4 \cdot \exp(-\alpha \theta u_k^2 / R^2)}{m \left[\left(\frac{1}{m} \right)^2 + u_k^2 \right] \cdot m^2 \cdot \left(\frac{1}{u_k^2} \right)} \quad (31)$	$\sum_{k=1}^{\infty} \frac{6 \cdot \exp(-\alpha \theta u_k^2 / R^2)}{m \left[\left(\frac{1}{m} \right)^2 - \left(\frac{1}{m} \right) + u_k^2 \right] \cdot \left(\frac{1}{u_k^2} \right)} \quad (33)$
E'_{av}	$\sum_{k=1}^{\infty} \frac{2 \cdot \exp(-\alpha \theta u_k^2 / R^2)}{m \left[\left(\frac{1}{m} \right)^2 + \left(\frac{1}{m} \right) + u_k^2 \right] \cdot \left(\frac{1}{u_k^2} \right)} \times \left[1 + 2m - \left(\frac{2}{u_k^2} \right) \right] \quad (30)$	$\sum_{k=1}^{\infty} \frac{4 \cdot \exp(-\alpha \theta u_k^2 / R^2)}{m \left[\left(\frac{1}{m} \right)^2 + u_k^2 \right] \cdot m^2 \cdot \left(\frac{1}{u_k^2} \right)} \times \left[1 + 2m - \left(\frac{4}{u_k^2} \right) \right] \quad (32)$	$\sum_{k=1}^{\infty} \frac{6 \cdot \exp(-\alpha \theta u_k^2 / R^2)}{m \left[\left(\frac{1}{m} \right)^2 - \left(\frac{1}{m} \right) + u_k^2 \right] \cdot \left(\frac{1}{u_k^2} \right)} \times \left[1 + 2m - \left(\frac{6}{u_k^2} \right) \right] \quad (34)$
Eq. of Volume Average Temperature t_{av}	$\frac{1}{R} \int_0^R t dr \quad (35)$	$\frac{2}{R^2} \int_0^R r t dr \quad (36)$	$\frac{3}{R^3} \int_0^R r^2 t dr \quad (37)$
Approximated t_{av}	$(t_s + 2t_0)/3 \quad (38)$	$(t_s + t_0)/2 \quad (39)$	$(3t_s + 2t_0)/5 \quad (40)$

necessary to change the heat flux of surface convection or radiation. Because the sudden temperature changes or the large temperature gradient in solids may cause the troubles or damages of materials due to the thermal stress.

It is the purpose of this report to present the charts for calculations of temperature distribution in solids when the surface conditions are changed stepwisely. One of the authors of this paper has already reported such charts for cylinders⁴⁾. This report contains the full charts for plates, cylinders and spheres in the wide range of parameters such as time, thickness of solid, thermal properties, and fluid or radiation heat transfer coefficient.

The charts for the constant surface temperature, which is the limit conditions of the infinite heat transfer coefficient, were also given. These full charts for plates, cylinders and spheres and for both initial conditions of the constant and parabolic temperature distributions had not be published.

All charts may be used not only for calculation of the heating or cooling operations but also for the mass transfer, for example, the drying of materials denoting the moisture content instead of the temperature.

Equations for calculation

Equations of heat conduction used in this report were summarized in Table 1. Equations (1), (2), and (3) are the one dimensional heat conduction equations of the semi-infinite plates with the thickness $2R$, the semi-infinite cylinders with radius R , and the spheres with radius R , respectively. Equation (4) denotes the initial conditions and means the parabolic temperature distribution in solids at the time $\theta=0$. This condition includes the case of the constant initial temperature when t_{oi} is equal to t_{si} , which was used in the already published charts¹⁾²⁾³⁾. The reason to use the parabolic initial temperature distribution conditions were described later. Equation (5) means that the temperature distributions are symmetric and that the temperature gradient is equal to zero at the center of $r=0$ for all solid shapes. Equation (6) gives the boundary conditions of $r=R$ and means that the heat conduction flux at the solid surface is equal to the rate of heat convection or radiation. The solutions of Equation (1), (2), or (3) with the boundary conditions of Equation (5) and (6) have already been given by Carslaw and Jaeger⁵⁾ for the general initial temperature distribution. These solutions could be represented in the form of Equation (7) for the parabolic initial temperature distribution, regardless of the solid shapes. E and E' were given in Equations (8) and (9) for the plate, Equations (10) and (11) for the cylinder, and Equations (12) and (13) for the sphere. For each solid shape, E is the solution for the constant initial temperature t_{oi} , which were used in the previous charts. When the initial temperature distribution is parabolic, the solutions are of the form that the second term $(t_{oi}-t_{si})/(t_{oi}-t^*)E'$ is subtracted from E . E and E' are given by the infinite series. The values of u_k in each term of the series are the k th positive root of Equation (14), (15), or (16) for each

shape.

The surface temperatures are obtained from the values of $r=R$ in the equations of E and E' . These values are shown in the column of E_s and E'_s in Table 1. The center temperatures are given also from the values of $r=0$ in the equations of E and E' for each shape and shown as E_0 and E'_0 in Table 1. The volume average temperature, which is equal to the mass average for the constant density, can be calculated by the Equation (35), (36), or (37) for each shape. E_{av} and E'_{av} for the average temperatures were obtained by the substitutions of Equations (8)~(13) for each shape, in Equation (7) and the integration in Equation (35), (36), or (37). If the temperature distributions at any time are approximately represented by the parabolic form of Equation (4), the average temperature can be expressed with the values of center and surface temperature as shown in Equation (38), (39), or (40) for each shape, which is obtained by the substitution of Equation (4) in Equation (35), (36), or (37).

Calculated results

E_s , E'_s , E_0 , E'_0 , E_{av} , and E'_{av} for plates, cylinders, and spheres were calculated for the various values of $m=\lambda/Rh$ and $\alpha\theta/R^2$. Calculations were carried out by the FACOM 231 computer of the Faculty of Engineering of Yamaguchi University. When the values of $\alpha\theta/R^2$ is less than 0.2, the conversion of series of E and E' becomes gradual, especially for large values of m . The series calculation were performed until the residual terms became less than 10^{-6} , which corresponds to the value of $u_k^2\alpha\theta/R^2$ in the series larger than 15.

Results of the calculations were shown in charts with dimensionless time $\alpha\theta/R^2$ as abscissa and E_s or E'_s as ordinate using the parameter of $1/m$. E_s , E'_s , E_0 , E'_0 , E_{av} and E'_{av} for the plate were shown in Fig. 1 (a~f). These values for the cylinder and the sphere were also shown in Fig. 2 (a~f) and Fig. 3 (a~f) respectively. In these charts, $\alpha\theta/R^2$ as abscissa was divided into 3 ranges, i.e., $0\sim 3$, $3\sim 10$, $10\sim 30$; and for each of the ranges the abscissa of $\alpha\theta/R^2$ changed the scale. E_0 , E_s , and E_{av} are the solutions of the constant initial temperature and are the same values given in the already published charts. The charts of E_s , E_0 , and E_{av} must accompany the charts of E'_s , E'_0 , and E'_{av} for the calculations of temperature histories in the case of stepwise change of surface convection or radiation conditions. These charts were all shown in the same scale covering the wide range of parameters.

In these charts, E and E' for intermediate values of $1/m$ can be read precisely by the interpolation of the plot for $\log E$ or $\log E'$ vs. $1/m$.

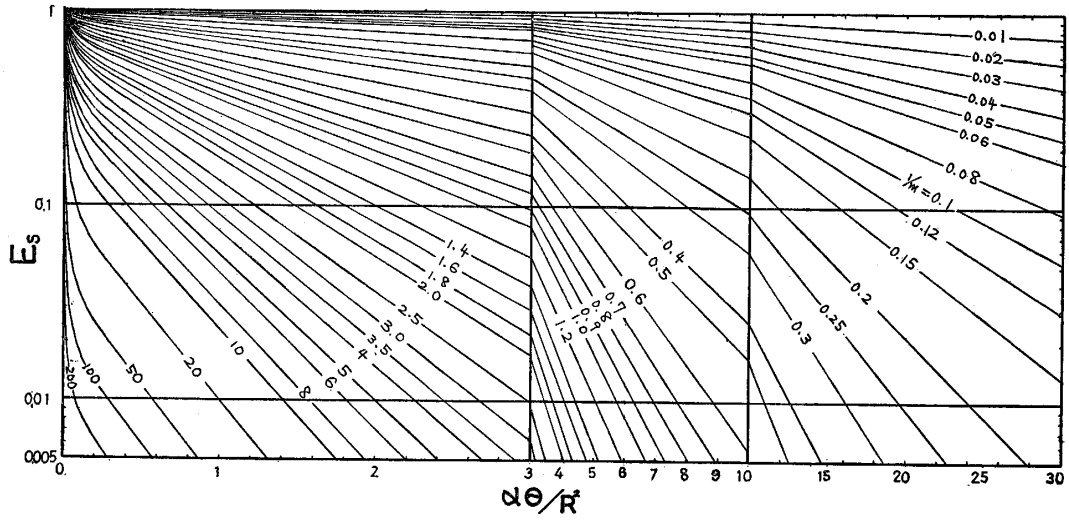


Fig. 1-a. E_s of plate

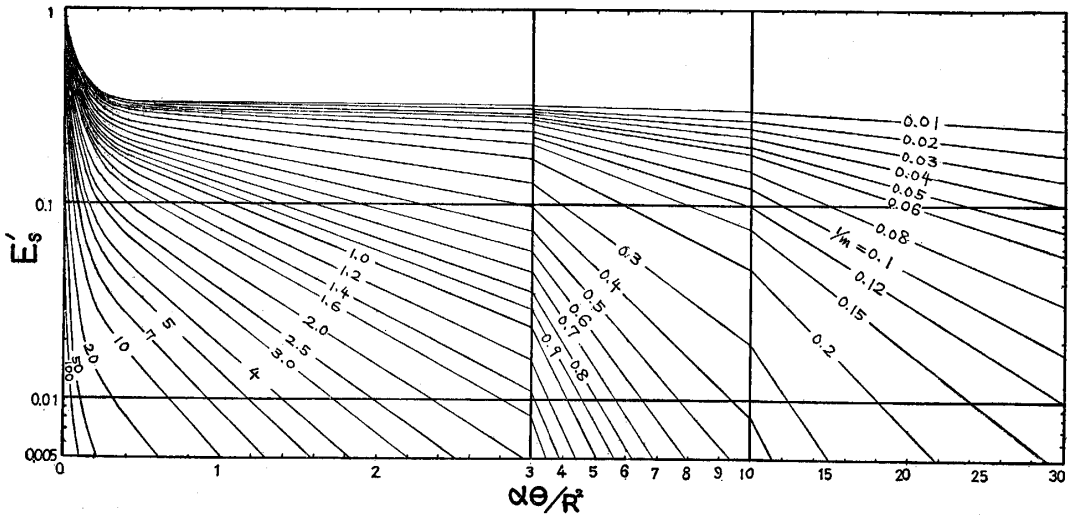


Fig. 1-b. E'_s of plate

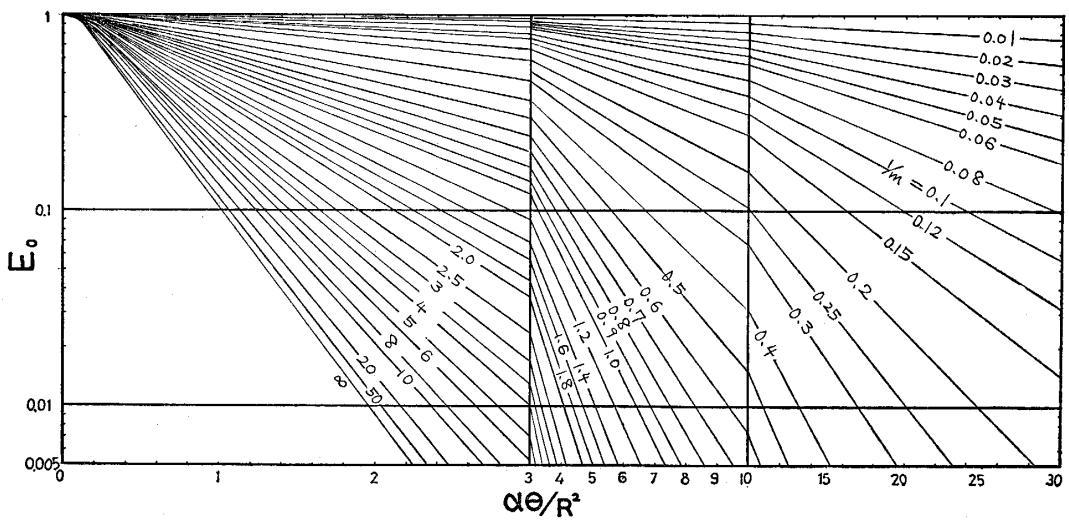


Fig. 1-c. E of plate

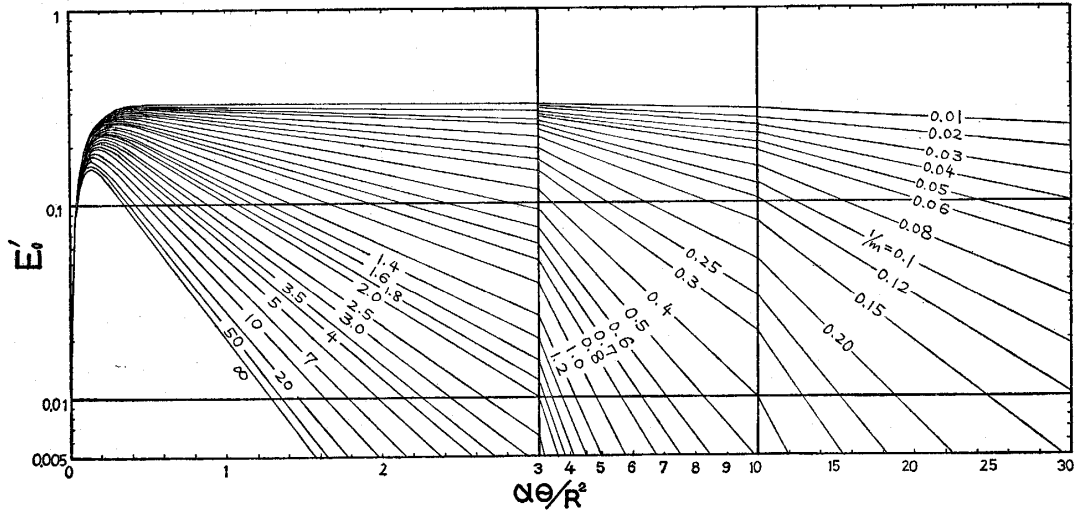


Fig. 1-d. E'_0 of plate

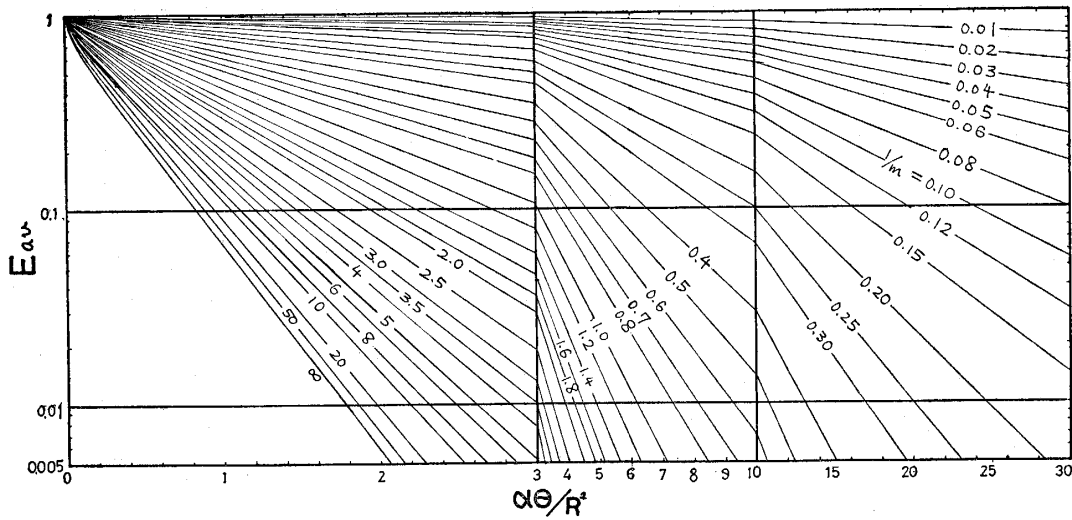


Fig. 1-e. E_{av} of plate

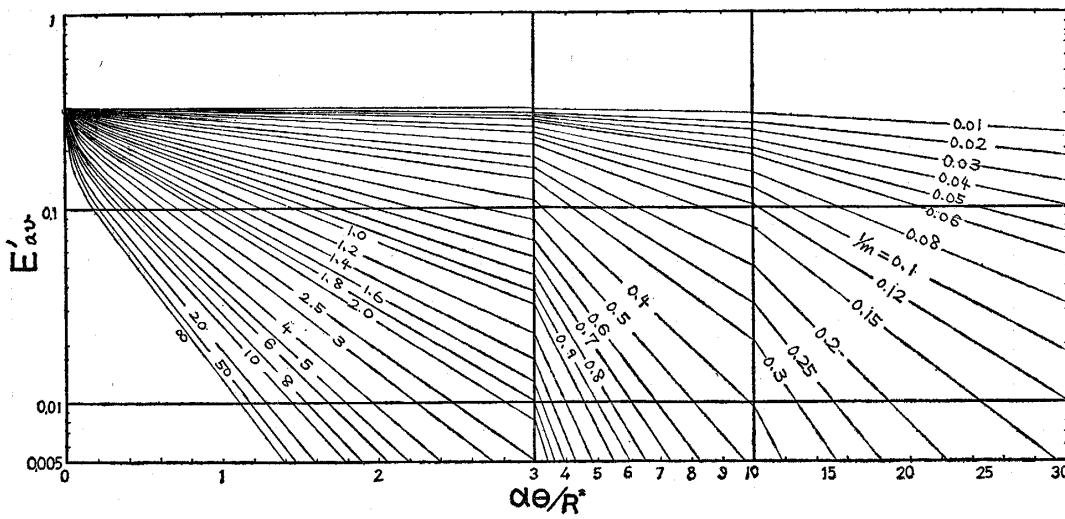


Fig. 1-f. E'_{av} of plate

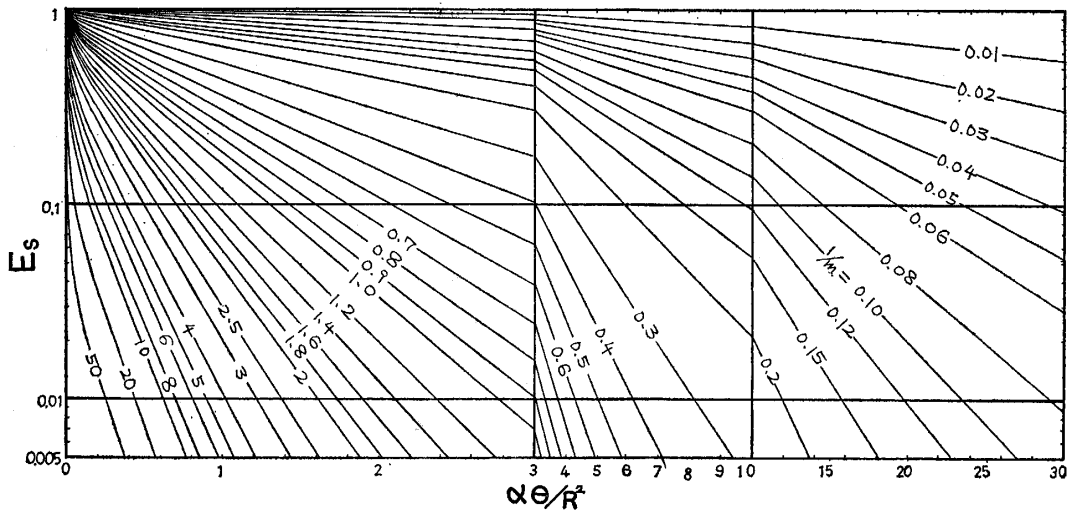


Fig. 2-a. E_s of cylinder

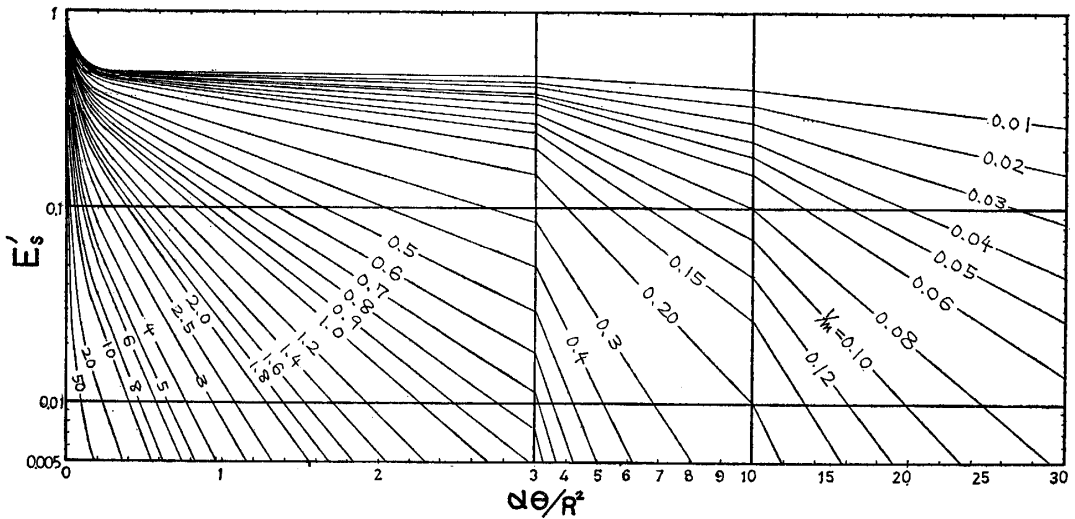


Fig. 2-b. E'_s of cylinder

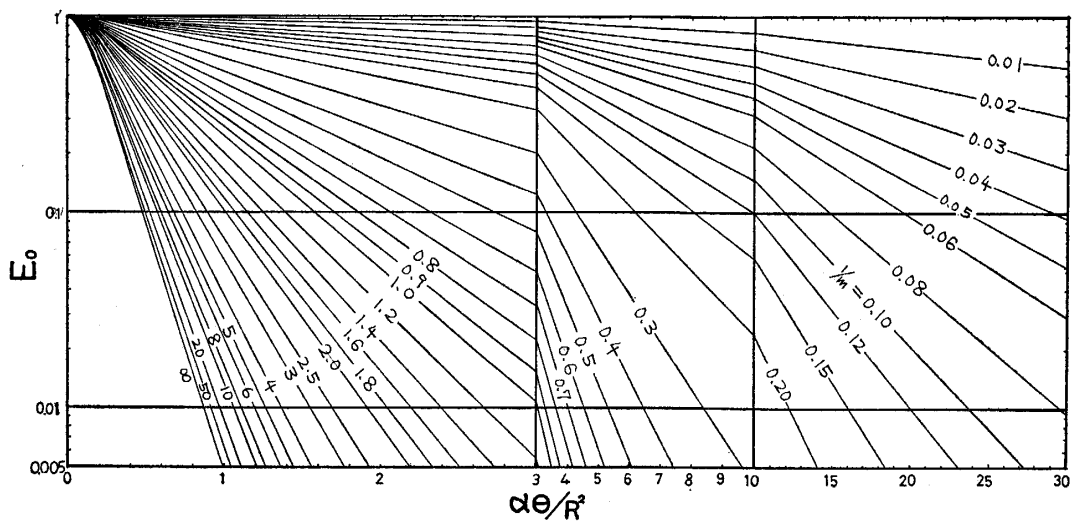


Fig. 2-c. E_0 of cylinder

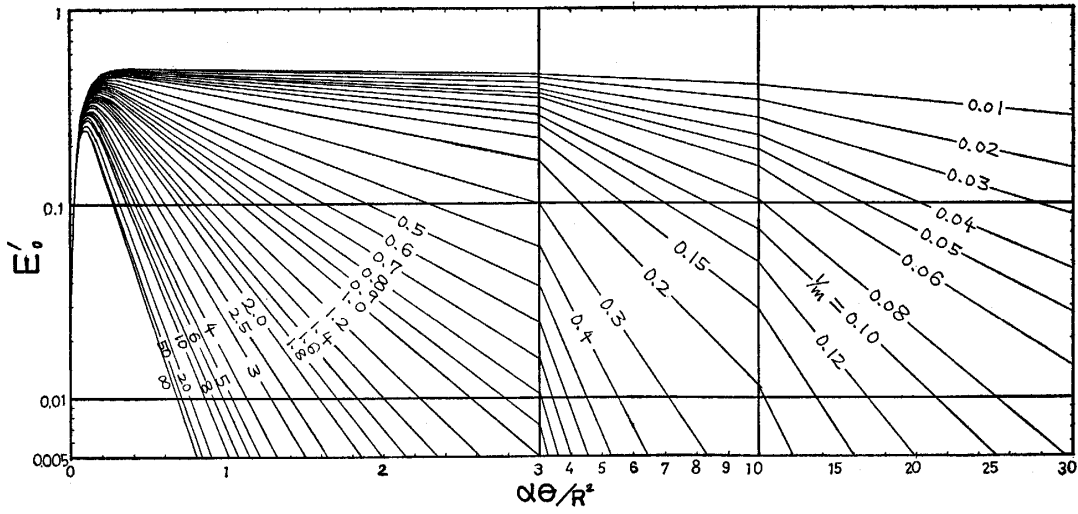


Fig. 2-d. E'_0 of cylinder

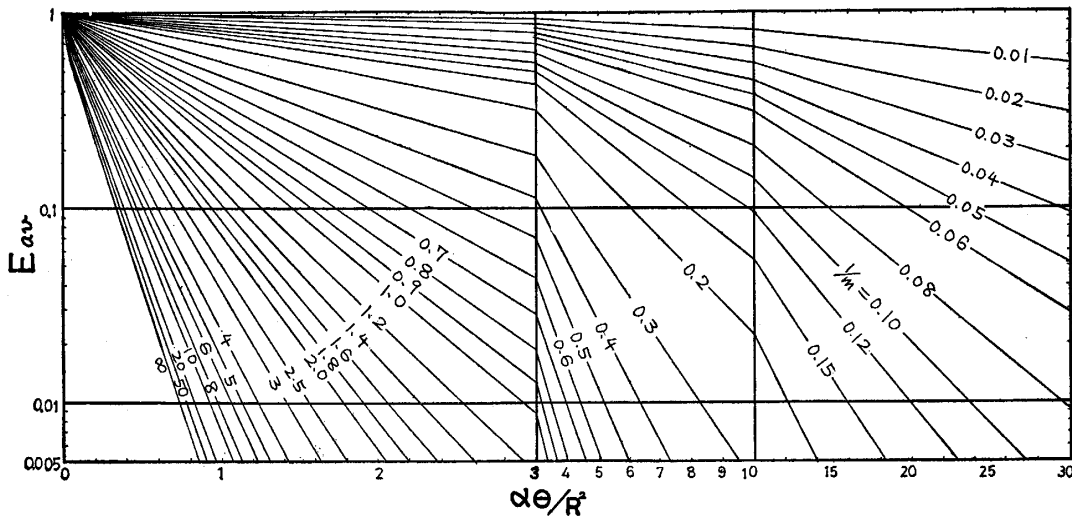


Fig. 2-e. E'_{av} of cylinder

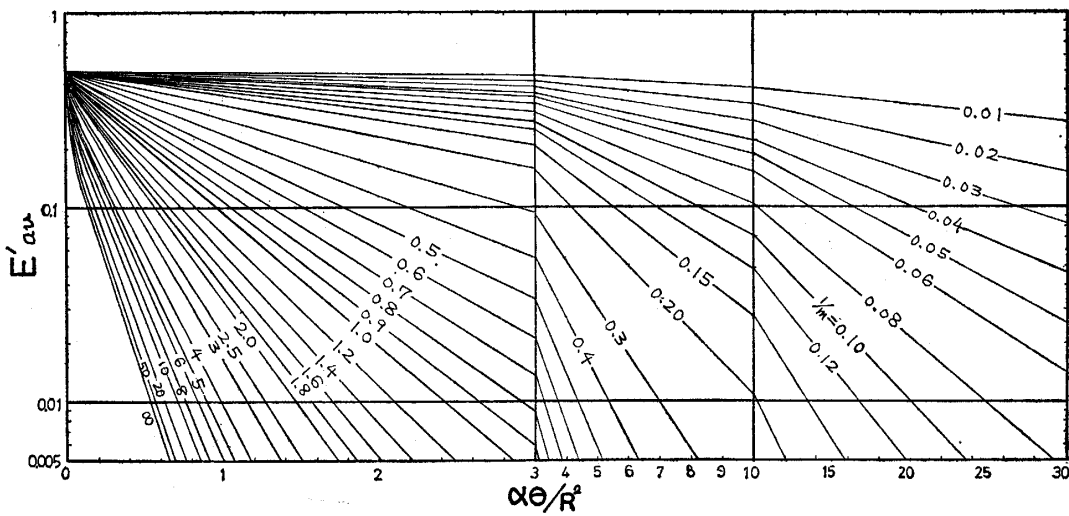


Fig. 2-f. E'_{av} of cylinder

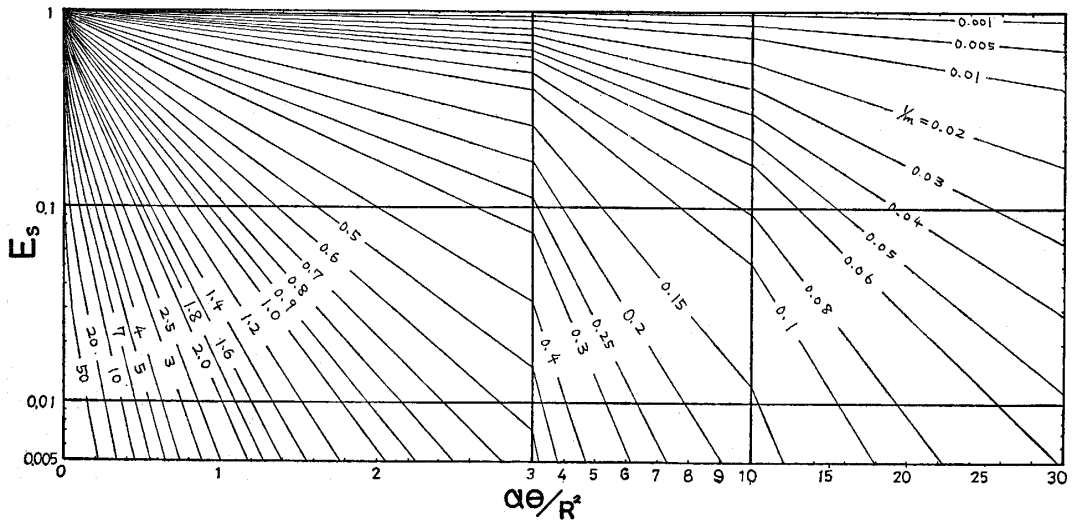


Fig. 3-a E_s of sphere

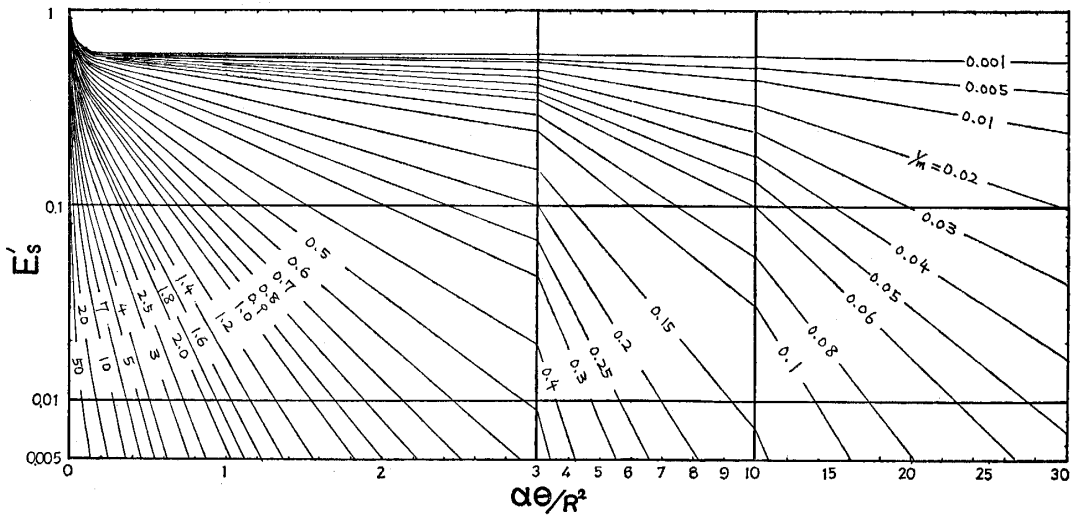


Fig. 3-b. E'_s of sphere

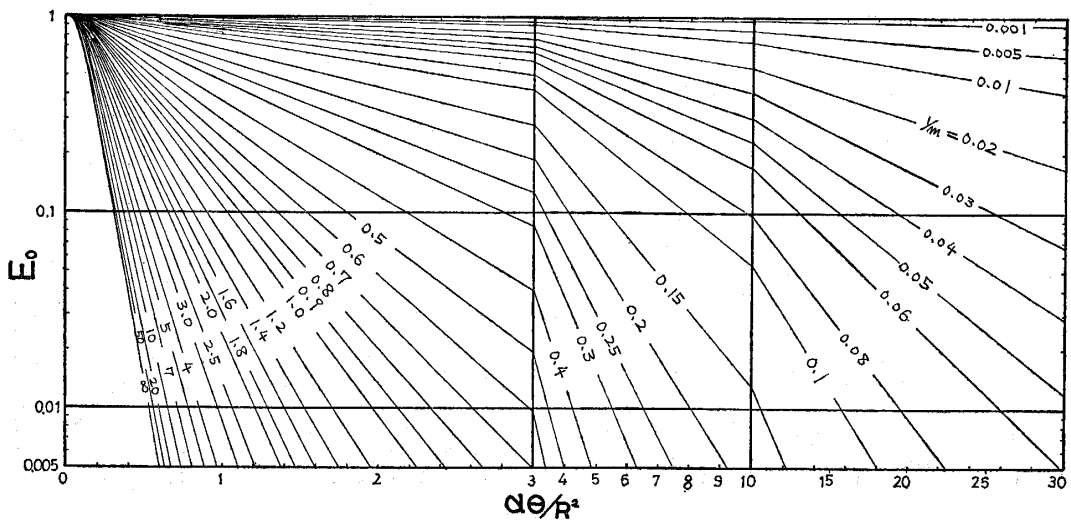


Fig. 3-c. E_0 of sphere

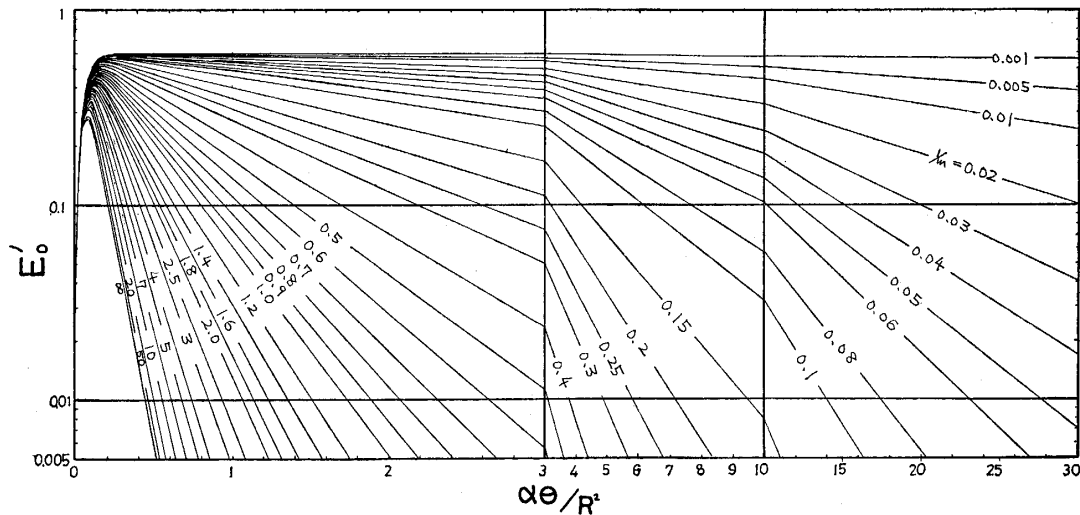


Fig. 3-d. E'_0 of sphere

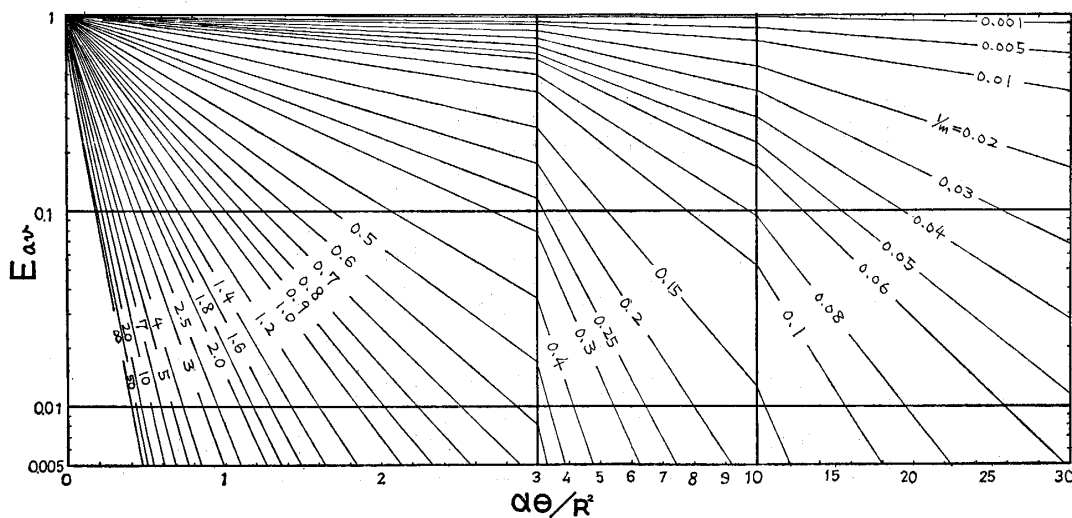


Fig. 3-e. E_{av} of sphere

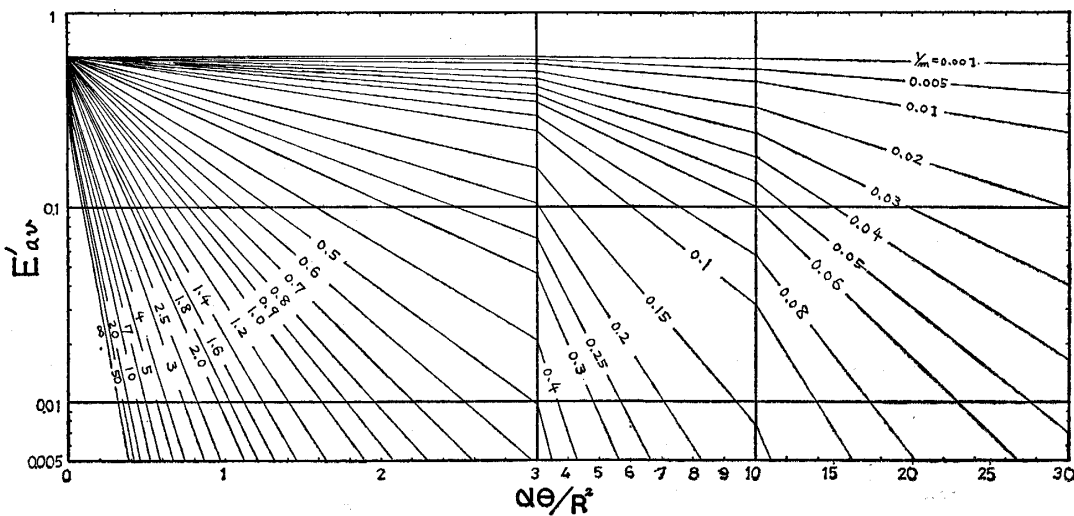


Fig. 3-f. E'_{av} of sphere

Temperature distributions

Temperature distributions in solids, as the dimensionless form at any time, can be shown from Equation (7) in the following equation:

$$\frac{t_s - t}{t_s - t_0} = \frac{(E_s - E) - p(E'_s - E')}{(E_s - E_0) - p(E'_s - E'_0)} \quad (41)$$

where

$$p = \frac{t_{oi} - t_{si}}{t_{oi} - t^*} \quad (42)$$

The initial temperature distribution conditions are classified into the following six cases from the values of p as illustrated in Fig. 4.

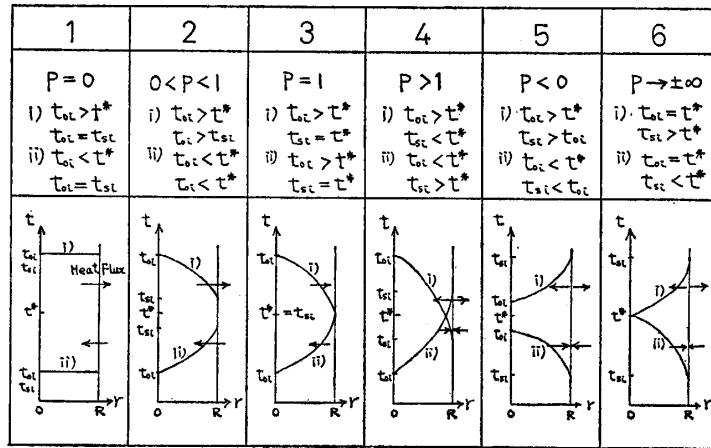


Fig. 4. Classification of the initial temperature distribution

1. $p=0$ In this case, the initial temperature is constant and uniform. If $t_{oi} - t^* > 0$, the solid is cooled, and if $t_{oi} - t^* < 0$, the solid is heated.

2. $0 < p < 1$ In this case, the initial temperature distribution is parabolic. If $t_{oi} - t^* > 0$, then $t_s > t^*$, and the solid is cooled. However if $t_{oi} - t^* < 0$, then $t_s < t^*$, the solid is heated.

3. $p=1$ With the parabolic initial temperature, the initial surface temperature is equal to the equilibrium temperature. But the surface temperature can not be held constant for $\theta > 0$, unless the heat transfer coefficient is infinite. The variations of the surface temperatures were shown with those of the center temperatures in Fig. 5. For example, when the solid is cooling, the surface temperature increases from the initial value of t^* for some time after the start of cooling, reaches to the maximum value, and then decreases again exponentially to the equilibrium temperature. The maximum temperature depends on m and the larger values of m give the larger maximum temperature. This means

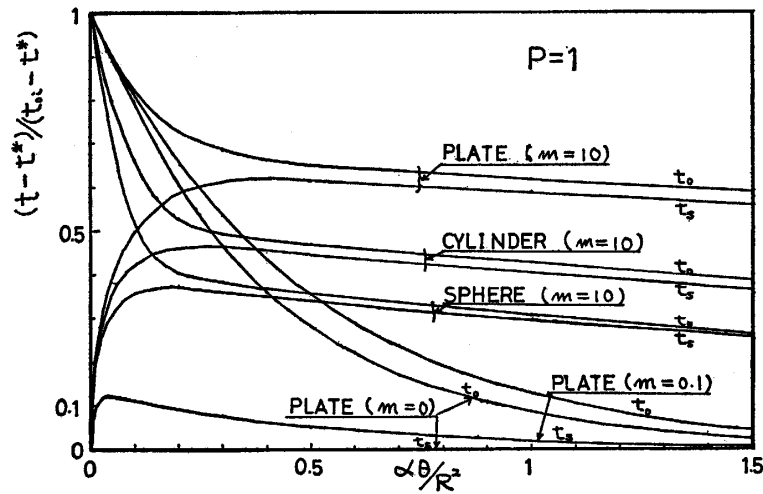


Fig. 5. Surface and center temperature change for $p=1$

that the heat flux of the inner part of the solid due to the temperature gradient is larger than the surface heat flux of convection or radiation in the initial period. The constancy of $t_s = t^*$ at any time can be held only when the surface heat flux is infinitely large. This case was discussed in the last section. The cases of 4, 5, and 6, in Fig. 4 are less interesting because these will be the rare cases in the practical operations. In these cases, the direction of the heat flux changes at the surface. In this report, the cases of 1, 2, and 3 in Fig. 4 were discussed.

In order to consider the temperature distributions in solids, the values of E and E' must be analyzed. The logarithmic values of E and E' in Fig. 1~3 show the linear changes with $\alpha\theta/R^2$ for the range of $\alpha\theta/R^2 > 0.3$. This means that the equations of E and E' converge rapidly, and for $\alpha\theta/R^2 > 0.3$, all terms after first can almost be neglected. If E and E' can be expressed with the first term alone, Equation (41) is reduced as follows for each shape, and the effect of the parameter p can be neglected.

For plates:

$$\frac{t_s - t}{t_s - t_0} = \frac{\cos(u_1 r/R) - \cos(u_1)}{1 - \cos(u_1)} \tag{43}$$

For cylinders:

$$\frac{t_s - t}{t_s - t_0} = \frac{J_0(u_1 r/R) - J_0(u_1)}{1 - J_0(u_1)} \tag{44}$$

For spheres:

$$\frac{t_s - t}{t_s - t_0} = \frac{\left(\frac{1}{r/R}\right) \sin(u_1 r/R) - \sin(u_1)}{u_1 - \sin(u_1)} \tag{45}$$

The functions of $\cos(x)$, $J_0(x)$, and $\sin(x)$ can be expressed in the form of series expansion.

$$\cos(x) = 1 - \frac{x^2}{2!} + \frac{x^4}{4!} - \frac{x^6}{6!} + \dots + (-1)^k \frac{x^{2k}}{(2k)!} \pm \dots \quad (46)$$

$$J_0(x) = 1 - \frac{x^2}{4} + \frac{x^4}{32} - \dots + (-1)^k \frac{(x/2)^{2k}}{(k!)^2} \pm \dots \quad (47)$$

$$\sin(x) = x - \frac{x^3}{3!} + \frac{x^5}{5!} - \dots + (-1)^k \frac{x^{2k+1}}{(2k+1)!} \pm \dots \quad (48)$$

Substitutions of Equation (46) into Equation (43) for plates, and respective substitutions of equations for cylinders and spheres, give the following approximate equations.

For plates:

$$\frac{t_s - t}{t_s - t_0} = \left[1 - \left(\frac{r}{R} \right)^2 \right] \cdot \frac{1 - \frac{u_1^2}{12} \left[1 + \left(\frac{r}{R} \right)^2 \right] + \frac{u_1^4}{360} \left[1 + \left(\frac{r}{R} \right)^2 + \left(\frac{r}{R} \right)^4 \right] - \dots}{1 - \frac{u_1^2}{12} + \frac{u_1^4}{360} - \dots} \quad (49)$$

For cylinders:

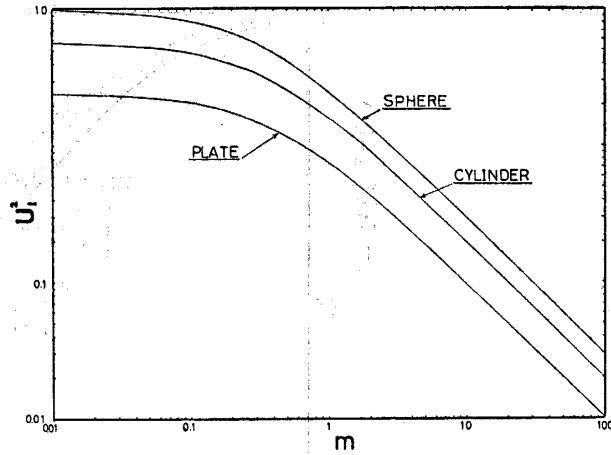
$$\frac{t_s - t}{t_s - t_0} = \left[1 - \left(\frac{r}{R} \right)^2 \right] \cdot \frac{1 - \frac{u_1^2}{8} \left[1 + \left(\frac{r}{R} \right)^2 \right] + \frac{u_1^4}{96} \left[1 + \left(\frac{r}{R} \right)^2 + \left(\frac{r}{R} \right)^4 \right] - \dots}{1 - \frac{u_1^2}{8} + \frac{u_1^4}{96} - \dots} \quad (50)$$

For spheres:

$$\frac{t_s - t}{t_s - t_0} = \left[1 - \left(\frac{r}{R} \right)^2 \right] \cdot \frac{1 - \frac{u_1^2}{20} \left[1 + \left(\frac{r}{R} \right)^2 \right] + \frac{u_1^4}{840} \left[1 + \left(\frac{r}{R} \right)^2 + \left(\frac{r}{R} \right)^4 \right] - \dots}{1 - \frac{u_1^2}{20} + \frac{u_1^4}{840} - \dots} \quad (51)$$

From Equation (49), (50), and (51), the dimensionless temperature distributions at any time can be reduced to the form of Equation (4) regardless of solid shapes when u_1 is small. The value of u_1 is the first root of Equation (14), (15), or (16) for each shape and is shown in Fig. 6 as the relation of u_1^2 and m . When the values of m tend to zero, u_1 converges to the value of $\left(\frac{2}{\pi} \right)$ for plates, 2.4048 ... which is the 1st root of $J_0(u_k) = 0$ for cylinders and π for spheres. When the values of m tend towards infinity, u_1 tends to zero and in the range of $m > 10$, u_1 can be expressed in the linear function of $1/m$ for each shape. This means that the temperature distribution tends to the parabolic equation of the temperature distribution to the parabolic equation as m tend towards infinity.

Fig. 6. The 1st root of Equation (14), (15) and (16)



In order to know the accuracy of approximation of the temperature distribution to the parabolic equation at any time, the strict values of $(t_s - t)/(t_s - t_0)$ were calculated from Equation (41).

The temperature distribution curves of $(t_s - t)/(t_s - t_0)$ vs. r/R depend on $\alpha\theta/R^2$, m , and p . The curves for $\alpha\theta/R^2=0.3$ were shown in Fig. 7, 8, and 9 for each shape. In these figures, the curves for $m=0.1$ are almost independent on p , but give lower values than the parabolic curve. The effects of p on the error of approximation become increasingly more predominant for the larger m . For $m=10$, the curve of $p=0$ is almost coincident with the parabolic curve, whereas the curve for $p=1$ deviates somewhat to a great extent. If $p=0$, the approximation of the parabolic equation becomes better for larger values of m .

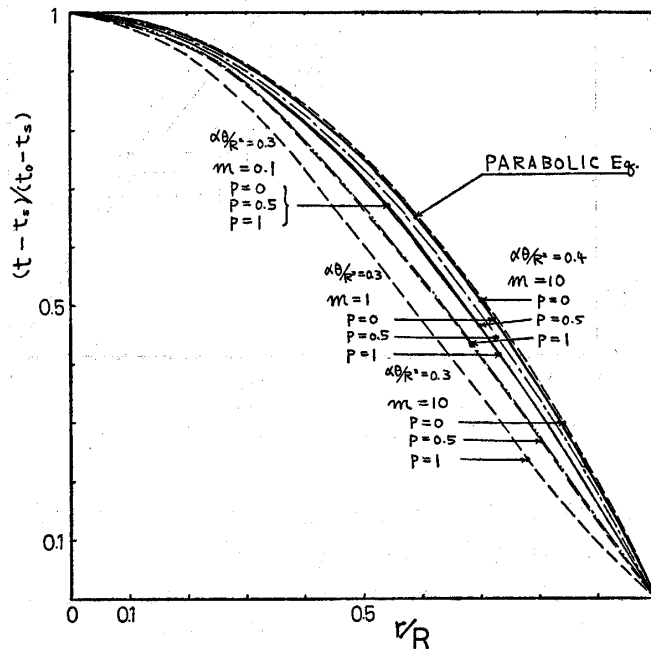


Fig. 7. Temperature distribution for plate

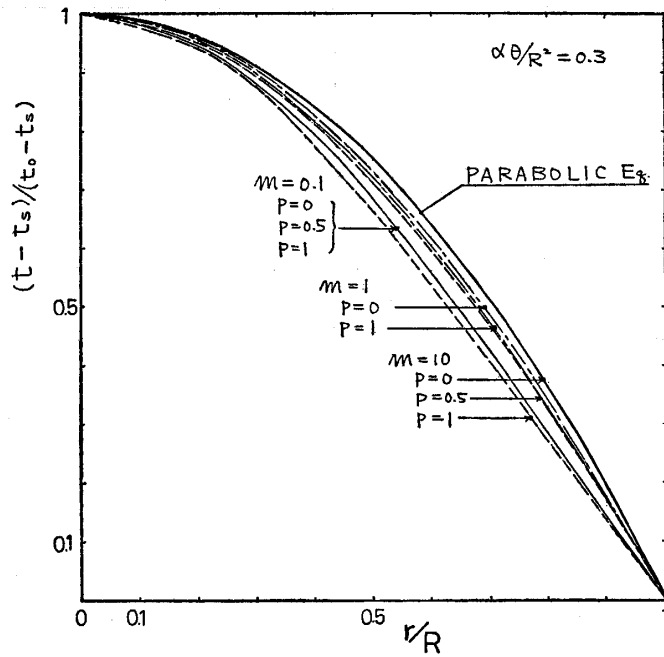


Fig. 8. Temperature distribution for cylinder

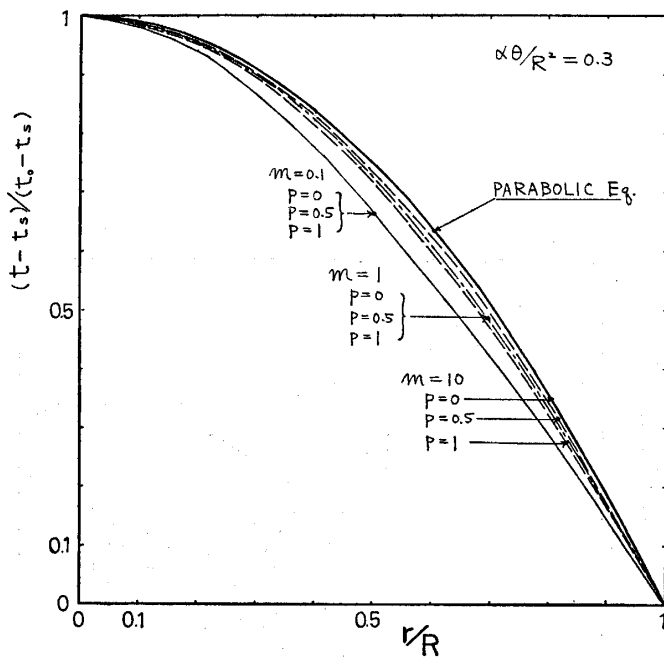


Fig. 9. Temperature distribution for sphere

For the curves of $\alpha\theta/R^2=0.4$, the deviation from the parabolic curve is much less than the deviation that for the curves of $\alpha\theta/R^2=0.3$; which means the approximation of the 1st term in the series is almost accomplished for larger values of m when $\alpha\theta/R^2=0.4$. The reason that the dependency of p becomes larger for larger values of m is due to the fact that the approximation of the 1st

term is insufficient because of the smaller values of u_1 for larger values of m as shown in Fig. 6.

In Fig. 10, 11 and 12, the temperature distribution curves for $p=0$ and $\alpha\theta/R^2=0.2$ were shown in the form of $(t-t^*)/(t_0-t^*)$, which was obtained by

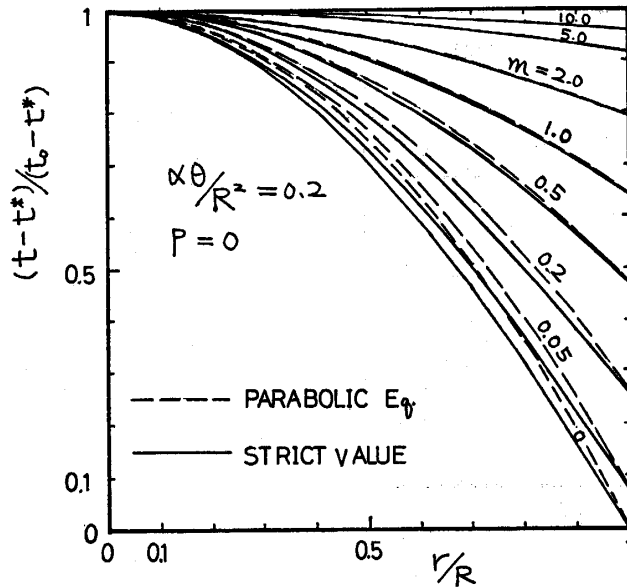


Fig. 10. Temperature distribution for $p=0$ (plate)

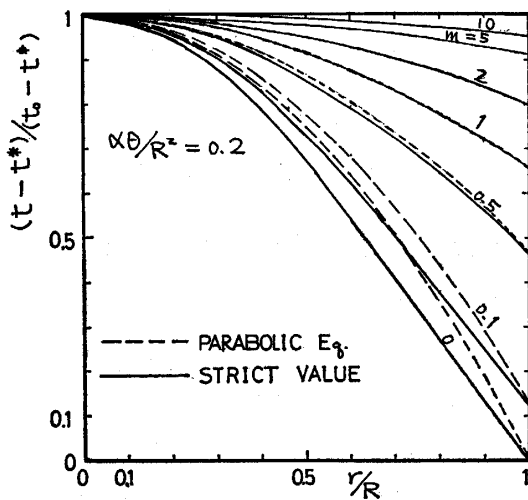


Fig. 11. Temperature distribution for $p=0$ (cylinder)

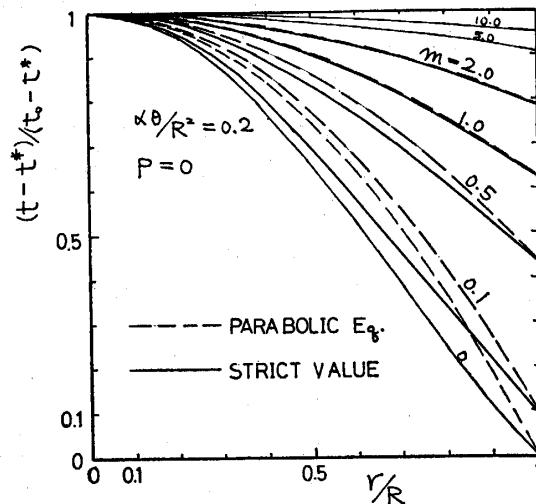


Fig. 12. Temperature distribution for $p=0$ (sphere)

E/E_0 . These figures show that the curve for $p=0$, namely the constant initial temperature, gives the good conformity of the parabolic distribution curve even for the small value of $\alpha\theta/R^2=0.2$. Another remark was that the distribution curve becomes flat for large values of m and for $m=10$, the difference between the surface temperature and the center one is 5% of that of the surface temperature and the equilibrium temperature. This corresponds with the ratio of the

external thermal resistance, $1/h$, to the overall internal thermal resistance, R/λ . Fig. 13 shows the asymptotic curves for large values of $\alpha\theta/R^2$ ($\alpha\theta/R^2 > 0.4$), in which the effect of p is negligible and depends only on the values of m .

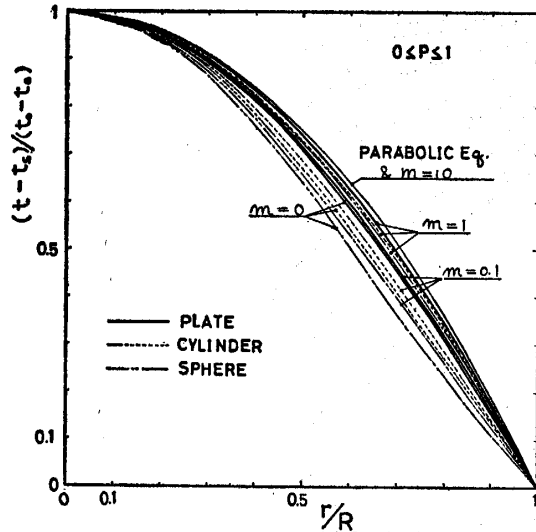


Fig. 13. Asymptotic curve of temperature distribution for large $\alpha\theta/R^2$ ($\alpha\theta/R^2 > 0.4$)

From these calculations of the temperature distribution, the following conclusions were obtained.

- 1) When $p=0$, $\alpha\theta/R^2 > 0.2$ and $m > 1$, the parabolic curves give the good approximation and when $1 < m < 0.1$, the fairly well approximation for $p=0$ and $\alpha\theta/R^2 > 0.2$.
- 2) When $0 \leq p \leq 1$ and $m > 1$, the parabolic curves give the good approximation for $\alpha\theta/R^2 > 0.4$. The approximation is improved rapidly for the larger values of $\alpha\theta/R^2$.
- 3) When $0.3 < \alpha\theta/R^2 < 0.4$, the approximation is good for $0 < p < 0.5$. The approximation is improved for the smaller values of p , and the deviation due to the values of p becomes larger for the larger values of m .
- 4) The asymptotic curve for the large values of $\alpha\theta/R^2$ varies with the values of m and independent on the values of p . For $m > 1$, the approximation of the parabolic equation is satisfactory. For $1 \geq m \geq 0.1$, the approximation is fairly well; and for $m < 0.1$ the approximation includes some errors, especially for the intermediate values of r/R .

The calculation method for the stepwise change of surface convection or radiation conditions

The conclusion in the foregoing section, that the temperature distribution at any time $\alpha\theta/R^2 > 0.2$ for $p=0$ can be approximated to the parabolic equation, gives the method for calculations of temperature histories when the surface heat convection or radiation conditions are changed stepwisely. When the solid,

which has uniform constant temperature initially, is heated or cooled by surface convection or radiation, the temperature distribution attain to the parabolic curve for the dimensionless time $\alpha\theta/R^2 > 0.2$ with the allowance of some error for the case of small values of m . The surface and center temperatures can be obtained from the charts for E_0 and E_s at the time $\alpha\theta/R^2 > 0.2$ when the surface convection or radiation conditions are changed. Then, these temperatures gives the initial condition in Equation (4) in the new heating or cooling period in which $0 \leq p \leq 1$, and the surface and center temperature changes for the new period can be calculated from the charts for E_0 , E'_0 , E_s and E'_s with Equation (7). The surface and center temperatures at any time for $\alpha\theta/R^2 > 0.4$, ($\alpha\theta/R^2 > 0.3$ with the allowance of some error for the large values of p when m is large), give the temperature distribution in the new period as the function of (r/R) according to the Equation (4). The average temperatures are calculated from the charts for E_{av} and E'_{av} . But more conveniently if the surface and center temperatures are given at any time, $\alpha\theta/R^2 > 0.4$, The average temperatures can be obtained from the arithmetic calculation of the Equation (38), (39), or (40) for each shape.

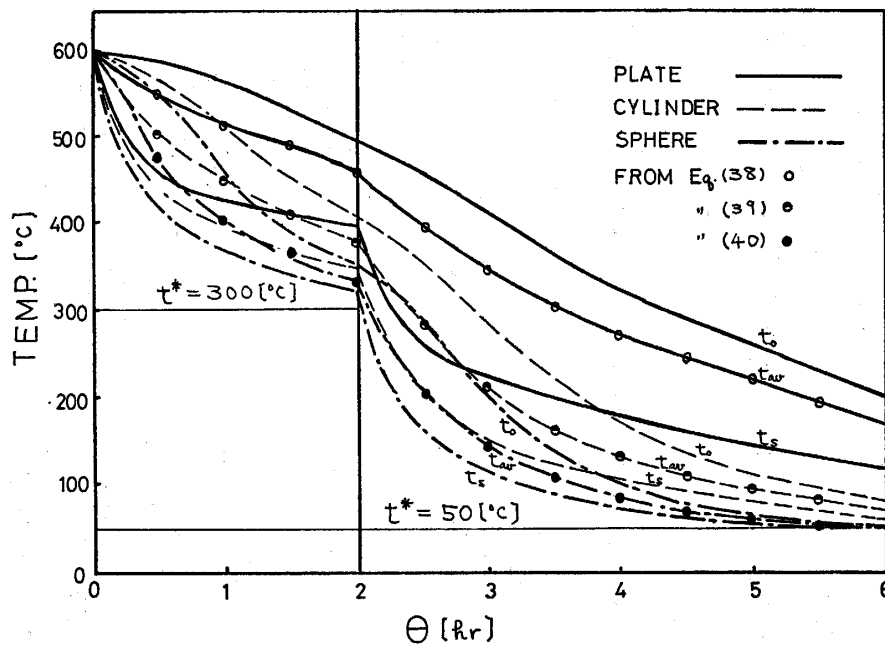


Fig. 14. The example of calculation

The use of charts and calculations were illustrated in the following examples.

The solid, with $R=10$ (cm), $\lambda=1$ (kcal/mhr°C), $C_p=0.2$ (kcal/kg°C), $\rho=2000$ (kg/m³) and the initial temperature $t_{oi}=t_{si}=600$ (°C), are cooled initially by the gas stream with the temperature $t^*=300$ (°C) for the time $\theta=2$ (hr) and then cooled by the gas stream of $t^*=50$ (°C) for $\theta=4$ (hr). The heat transfer coefficient is $h=20$ (kcal/m²hr°C). The temperature histories were calculated for the center, surface, and average temperature for the shape of plate, cylinder and sphere, respectively. Results were shown in Fig. 14. The average

Table 2. The equations for the condition of the infinite heat transfer coefficient

Shape	Plate	Cylinder	Sphere
Boundary condition-2'	$t_s = t^*$	$r = \pm R$	$(h \rightarrow \infty, m \rightarrow 0)$
E	(53) $\sum_{k=1}^{\infty} \frac{(-1)^{k+1}}{4} \cdot \frac{\exp(-\alpha\theta u_k^2/R^2) \cos(u_k r/R)}{(2k-1)\pi}$	(55) $\sum_{k=1}^{\infty} \frac{2 \cdot \exp(-\alpha\theta u_k^2/R^2)}{u_k J_1(u_k)} J_0(u_k r/R)$	(57) $\sum_{k=1}^{\infty} \frac{2}{r/R} \cdot \frac{(-1)^{k+1}}{k\pi} \cdot \exp(-\alpha\theta u_k^2/R^2) \sin(u_k r/R)$
E'	(54) $\sum_{k=1}^{\infty} \frac{(-1)^{k+1}}{4} \cdot \frac{\exp(-\alpha\theta u_k^2/R^2) \cos(u_k r/R)}{(2k-1)\pi} \times \left[1 - \frac{8}{(2k-1)^2 \pi^2} \right]$	(56) $\sum_{k=1}^{\infty} \frac{2 \cdot \exp(-\alpha\theta u_k^2/R^2) J_0(u_k r/R)}{u_k J_1(u_k)} \times \left[1 - \frac{4}{u_k^2} \right]$	(58) $\sum_{k=1}^{\infty} \frac{2}{r/R} \cdot \frac{(-1)^{k+1}}{k\pi} \cdot \exp(-\alpha\theta u_k^2/R^2) \cdot \sin(u_k r/R) \times \left[1 - \frac{6}{k^2 \pi^2} \right]$
u_k	(59) $\frac{2k-1}{2} \pi$	(60) $J_0(u_k) = 0$	(61) $k\pi$
E_s, E'_s	0	0	0
E_0	(62) $\sum_{k=1}^{\infty} \frac{(-1)^{k+1}}{4} \cdot \frac{\exp(-\alpha\theta u_k^2/R^2)}{(2k-1)\pi}$	(64) $\sum_{k=1}^{\infty} \frac{2 \cdot \exp(-\alpha\theta u_k^2/R^2)}{u_k J_1(u_k)}$	(66) $\sum_{k=1}^{\infty} \frac{(-1)^{k+1}}{6} \cdot 2 \cdot \exp(-\alpha\theta u_k^2/R^2)$
E'_0	(63) $\sum_{k=1}^{\infty} \frac{(-1)^{k+1}}{4} \cdot \frac{\exp(-\alpha\theta u_k^2/R^2)}{(2k-1)\pi} \times \left[1 - \frac{8}{(2k-1)^2 \pi^2} \right]$	(65) $\sum_{k=1}^{\infty} \frac{2 \cdot \exp(-\alpha\theta u_k^2/R^2)}{u_k J_1(u_k)} \left[1 - \frac{4}{u_k^2} \right]$	(67) $\sum_{k=1}^{\infty} \frac{(-1)^{k+1}}{6} \cdot 2 \cdot \exp(-\alpha\theta u_k^2/R^2) \times \left[1 - \frac{6}{k^2 \pi^2} \right]$
E_{av}	(68) $\sum_{k=1}^{\infty} \frac{8 \cdot \exp(-\alpha\theta u_k^2/R^2)}{(2k-1)^2 \pi^2}$	(70) $\sum_{k=1}^{\infty} \frac{4 \cdot \exp(-\alpha\theta u_k^2/R^2)}{u_k^2}$	(72) $\sum_{k=1}^{\infty} \frac{6 \cdot \exp(-\alpha\theta u_k^2/R^2)}{k^2 \pi^2}$
E'_{av}	(69) $\sum_{k=1}^{\infty} \frac{8 \cdot \exp(-\alpha\theta u_k^2/R^2)}{(2k-1)^2 \pi^2} \times \left[1 - \frac{8}{(2k-1)^2 \pi^2} \right]$	(71) $\sum_{k=1}^{\infty} \frac{4 \cdot \exp(-\alpha\theta u_k^2/R^2)}{u_k^2} \left[1 - \frac{4}{u_k^2} \right]$	(73) $\sum_{k=1}^{\infty} \frac{6 \cdot \exp(-\alpha\theta u_k^2/R^2)}{k^2 \pi^2} \times \left[1 - \frac{6}{k^2 \pi^2} \right]$

Table 2. continued

$\frac{t_{av} - t^*}{t_{avi} - t^*}$	$\sum_{k=1}^{\infty} \frac{8 \cdot \exp(-\alpha \theta u_k^2 / R^2)}{(2k-1)^2 \pi^2} \times \left[1 - p + \frac{8p}{(2k-1)^2 \pi^2} \right]$ <p style="text-align: right;">(74)</p>	$\sum_{k=1}^{\infty} \frac{4 \cdot \exp(-\alpha \theta u_k^2 / R^2)}{u_k^2} \times \left[1 - p + \frac{4p}{u_k^2} \right]$ <p style="text-align: right;">(75)</p>	$\sum_{k=1}^{\infty} \frac{6 \cdot \exp(-\alpha \theta u_k^2 / R^2)}{k^2 \pi^2} \times \left[1 - p + \frac{6p}{k^2 \pi^2} \right]$ <p style="text-align: right;">(76)</p>
$\frac{t_{av} - t^*}{t_{avi} - t^*} \text{ for } p=0$	E_{av}		
$\frac{t_{av} - t^*}{t_{avi} - t^*} \text{ for } p=1$	$\sum_{k=1}^{\infty} \frac{96 \cdot \exp(-\alpha \theta u_k^2 / R^2)}{(2k-1)^4 \pi^4}$ <p style="text-align: right;">(77)</p>	$\sum_{k=1}^{\infty} \frac{32 \cdot \exp(-\alpha \theta u_k^2 / R^2)}{u_k^4}$ <p style="text-align: right;">(78)</p>	$\sum_{k=1}^{\infty} \frac{90 \cdot \exp(-\alpha \theta u_k^2 / R^2)}{k^4 \pi^4}$ <p style="text-align: right;">(79)</p>

temperatures obtained from Equation (38), (39), or (40) were coincident with those obtained from the charts of E_{av} and E'_{av} for each shape.

Calculations for the constant surface temperature

When the heat transfer coefficient becomes larger, the surface temperature approaches to the equilibrium temperature immediately after the start of heating or cooling. The limit condition, that the heat transfer coefficient tends towards infinity, in which m tends to zero, gives the constant surface temperature of the equilibrium. Equations of this case were summarized in Table 2. The boundary condition of Equation (6) becomes Equation (52). The solutions of (1) (2) or (3) with Equations (4), (5), and (52) were popular, and here these were given in the form of Equation (7), obtained from Equations from Table 1 for $m \rightarrow 0$. E_s and E'_s were zero in this case. E_0 , E'_0 , E_{av} and E'_{av} were given in Fig. 1~3 as the values for $1/m = \infty$. For the average temperatures, Equation (74), (75), and (76) were given in the form of $(t_{av} - t^*) / (t_{av_i} - t^*)$, where t_{av_i} is the initial average temperature, and obtained from Equations (38), (39), and (40) in Table 1. Equations of $(t_{av} - t^*) / (t_{av_i} - t^*)$ for $p=0$ and $p=1$ were also given in Table 2. The charts for $(t_{av} - t^*) / (t_{av_i} - t^*)$ were shown in Fig. 15, which is often used for the calculation of the second drying rate period, but not given for the full form in the handbook.⁶⁾

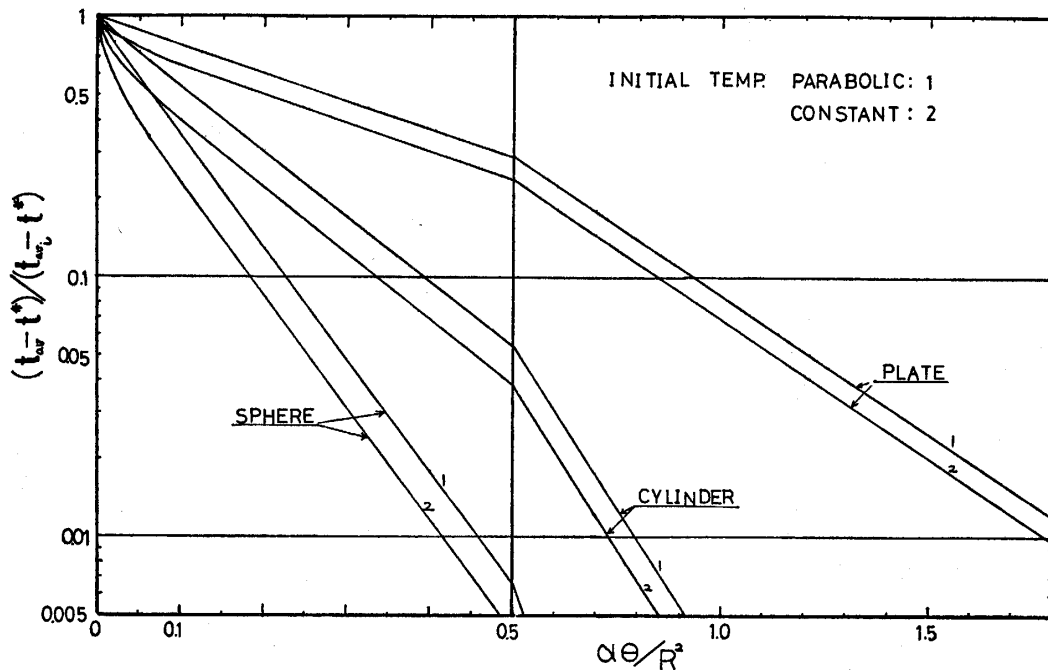


Fig. 15. $(t_{av} - t^*) / (t_{av_i} - t^*)$ for $t_s = t^*$

Conclusions

The charts for heat conduction problems with the parabolic initial tempera-

ture distribution, including the case of constant initial temperature, with the surface convection or radiation, were obtained for plates, cylinders, and spheres as shown in *Fig. 1~3*. The temperature distributions were able to be approximated by the parabolic form for $\alpha\theta/R^2 > 0.2$ $p=0$ and $m > 0.1$, in each shape and from this fact the calculation method of temperature histories for the stepwise change of the surface heat transfer conditions, were derived. The charts for average temperatures in the case of the constant surface temperature were also given.

Nomenclature

C_p	: specific heat of solid [kcal/kg°C]
h	: heat transfer coefficient [kcal/m ² hr°C]
m	: λ/Rh [—]
p	: $(t_{oi} - t_{si}) / (t_{oi} - t^*)$ [—]
R	: radius or thickness of solid [m]
r	: distance from the center [m]
t	: temperature [°C]
α	: $\lambda/\rho C_p$ [m ² /hr]
θ	: time [hr]
λ	: thermal conductivity [kcal/mhr°C]
ρ	: density [kg/m ³]
suffix	* : equilibrium value
	o : center value
	s : surface value
	av: average value
	i : initial value

References

- 1) H. P. Gurney and J. Lurie: *Ind. Eng. Chem.* **15**, 1170 (1923)
- 2) M. P. Heisler: *Trans. A.S.M.E.* **69**, 227 (1947)
- 3) H. C. Hottel: W. H. McAdams: "*Heat Transmission*" 3rd ed. p. 36 McGraw-Hill, New York (1954)
- 4) Y. Sano and S. Nishikawa: *Chem. Eng. (Japan)* **29**, 1034 (1965) (in Japanese)
- 5) H. S. Carslaw and J. C. Jaeger: "*Conduction of Heat in Solids*" 2nd ed. p. 114, 201 & 247, Oxford. (1947)
- 6) *Handbook for Chem. Eng. (Japan)*: edited by J.S.C.E. p. 638 (1968) (in Japanese)